JACS
JOURNAL OF THE AMERICAN CHEMICAL SOCIETY
Communication
pubs.acs.org/JACS

Role of Dimerization Efficiency of Transmembrane Domains in Activation of Fibroblast Growth Factor Receptor 3

Pavel E. Volynsky,[†,∥] Anton A. Polyansky,*[,†,‡,∥] Gulfia N. Fakhrutdinova,[†] Eduard V. Bocharov,[†] and Roman G. Efremov[†,§]

[†]M. M. Shemyakin and Yu. A. Ovchinnikov Institute of Bioorganic Chemistry, Russian Academy of Sciences, Moscow, 117997, Russia
[‡]Department of Structural and Computational Biology, Max F. Perutz Laboratories, University of Vienna, Campus Vienna Biocenter 5, Vienna, AT-1030, Austria
[§]Moscow Institute of Physics and Technology (State University), Dolgoprudny, Moscow Region, 141700, Russia

Supporting Information

ABSTRACT: Mutations in transmembrane (TM) domains of receptor tyrosine kinases are shown to cause a number of inherited diseases and cancer development. Here, we use a combined molecular modeling approach to understand molecular mechanism of effect of G380R and A391E mutations on dimerization of TM domains of human fibroblast growth factor receptor 3 (FGFR3). According to results of Monte Carlo conformational search in the implicit membrane and further molecular dynamics simulations, TM dimer of this receptor is able to form a number of various conformations, which differ significantly by the free energy of association in a full-atom model bilayer. The aforementioned mutations affect dimerization efficiency of TM segments and lead to repopulation of conformational ensemble for the dimer. Particularly, both mutations do not change the dimerization free energy of the predominant (putative "non-active") symmetric conformation of TM dimer, while affect dimerization efficiency of its asymmetric ("intermediate") and alternative symmetric (putative "active") models. Results of our simulations provide novel atomistic prospective of the role of G380 and A391E mutations in dimerization of TM domains of FGFR3 and their consecutive contributions to the activation pathway of the receptor.

The human fibroblast growth factor receptors (FGFRs) belong to the family of receptor tyrosine kinases (RTKs). Transmembrane (TM) domains of these proteins are comprised of a single helix and shown to play a crucial role in dimerization and/or activation of RTKs by controlling orientation of the intracellular kinase domains.[1] Single-point mutations in RTK TM domains are known to cause a number of diseases, while the mechanism of such effects is still under debate. In particular, the most frequent pathogenic mutations G380R and A391E in TM region of FGFR3 are associated both with oncogenesis and with disorders in skeletal development, causing lethal dysplasia and the Crouzon syndrome with acanthosis nigricans, respectively.[2,3] The G380R and A391E mutations are considered to stabilize FGFR3 dimerization in the cell membrane, resulting in uncontrollable signal transduction and emergence of pathology.[4,5] In addition, it was shown that these mutations have rather minor influence on dimerization efficiency of TM domains of FGFR3 in liposome assays using Förster resonance energy transfer (FRET) measurements,[6,7] while the detailed atomic picture of the observing effects is still unclear.

Here, we use a combined molecular modeling approach in order to explore possible conformational heterogeneity of FGFR3 TM dimer and estimate the effect of G380R and A391E mutations on thermodynamic characteristics of a conformational ensemble of the dimer. We address these questions using Monte Carlo (MC) conformational search in the implicit water-cyclohexane slab and subsequent molecular dynamics (MD) relaxation of the resulting dimer conformations in full-atomic membranes, followed by calculations of the association free energies (details in SI).

Results of MC calculations clearly show that the wild-type (WT) FGFR3 TM helices (Table S1) predominantly form left-handed dimeric conformations (positive values of the crossing angle χ), where mutual orientations of helices cover a wide range of rotational angles ($\alpha 1$, $\alpha 2$) around helix axes of the monomers (Figures 1a and S2). The most populated helix−helix interface I1 is formed by aromatic Y373, F383, F384 and aliphatic V372, I376, I386 residues (Figure 1b). This corresponds to one symmetrical model (s1, Figure 1c, top panel) and all asymmetrical ones. We should note that the symmetric conformation s1 corresponds well to TM dimer structure recently obtained by NMR spectroscopy in micellar medium (PDB code: 2LZL, backbone root-mean-square deviation (RMSD) between MC and experimental models is 2.2 Å, Figure S3). The alternative interface I2 includes polar patch formed by G375, S378, Y379, and G382 residues (Figure 1b) that is realized in the second symmetric model (s2, Figure 1c, bottom panel). In the majority of asymmetric models helices interact via I1 and I2 regions. The only right-handed dimer conformation ($\chi = -35°$) also belongs to this subset (a3, Figure 1c, middle panel). In addition, one of the left-handed asymmetric dimer conformations reveals a hybrid interface formed by the surface regions I1 and I3 (Figure 1b).

MC calculations for A391E mutant give an ensemble of dimer conformations, which is very similar to that in WT (Figure S2). In contrast, G380R substitution leads to an ensemble with a

Received: February 2, 2013
Published: May 16, 2013

dx.doi.org/10.1021/ja4011942 | J. Am. Chem. Soc. 2013, 135, 8105−8108

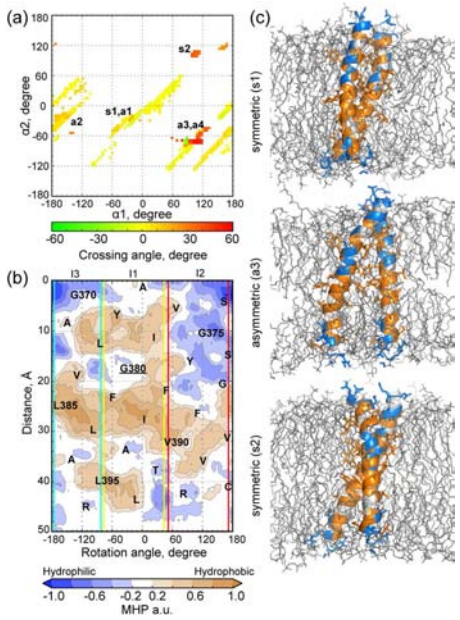

Figure 1. Conformational heterogeneity of FGFR3 TM dimer. (a) Maps of interfacial angles (α1, α2) of the lowest energy conformers obtained by MC conformational search in the implicit membrane of width 35 Å. α is the rotation angle around helix axis of the monomer. The map is colored with respect to values of helix−helix crossing angles according to the scale given below. Locations of different conformations of TM dimer are indicated. (b) 2D isopotential map of the molecular hydrophobicity potential (MHP) on the peptide surface (details in SI). Dimerization interfaces (I1, I2, and I3) are shown with vertical lines. (c) Representative dimer conformations after MD relaxation in POPC bilayer. In s1, s2, and a3 conformations TM helices interact via I1/I1, I2/I2 and I1/I2 interfaces, respectively. Peptides are shown with sticks and cartoon representation and colored according to hydrophobic properties of residues (MHP values). Lipids are shown with gray sticks.

larger number of asymmetric models as compared to WT (Figure S2).

For WT dimer we selected 6 models, which significantly differ in the interaction interfaces and packing geometry. Analogous models were also selected for A391E and G380R dimers. These 18 representative conformations were subjected to further 50 ns MD relaxation in full-atomic palmitoyloleoylphospatidyl-choline (POPC) bilayer, which was chosen in order to have a model system similar to that used in previous experimental studies of association of FGFR3 TM domains[6,7].

In the result of MD simulations, WT dimer conformations undergo minor structural rearrangements due to adaptation to the lipid environment. For most of the simulated models we observe small (by several degrees) changes in the crossing angle (Table S1), tilting of the helices with respect to the bilayer normal and variations in their mutual orientation (rotation angles α). This corresponds to the backbone RMSDs from the initial MC conformation in the range of 2.0−2.5 Å (Table S1, Figure S4). Asymmetric models a1 and a2 display the most prominent conformational changes during relaxation, which can be characterized by rotation of single (a2) or both (a1) helices with respect to the initial structure (Table S1, Figure S4).

Introduction of such strong mutations as addressed here destabilizes initial MC conformation of the dimers, obtained in the implicit membrane. We speculate that this effect is mostly associated with a strong impact of the explicit lipid environment, which is more sensitive to the presence of polar substitutions in the hydrophobic region of the bilayer. For instance, in agreement with previous observations,[8] introduction of Arg in the N-terminal part of TM helix in most cases leads to partial emersion of the whole dimers, which is demonstrated by a shift of the center of mass of the dimer along the bilayer normal (h, Table S1). Interestingly, Arg also induces additional stacking pair formation in a case, where it resides in the interfacial region (st, Table S1). In contrast, the effect of Glu mutation is less straightforward. Although the conformational dynamics of the dimer is quite similar to WT, the presence of Glu facilitates deeper water penetration into the membrane core and formation of interhelical hydrogen bonds.

While upon mutations both left-handed symmetric conformations and the asymmetric right-handed one (a3) remain close to the initial membrane bound MC conformations of the native dimers (backbone RMSD < 3.0 Å, Table S1), left-handed structures (a1, a2, a4) undergo more dramatic changes. Particularly, Arg substitution in all the cases perturbs significantly the dimer structure. The effect of A391E mutation here is more complex: it makes the dimer conformation a1 close to s1 of WT (RMSD is 2.9 Å, Table S2) as well as both a2 and a4 close to each other (RMSD is 2.8 Å, Table S2), while the latter totally changes its packing with respect to WT a4 model. Thus, the fact that FGFR3 dimer can adopt a number of different conformations in the membrane as we have also seen previously for other RTKs[9] makes possible a scenario, when the considered mutations do not induce strong structural rearrangements of the "main" symmetric dimer states (s1, s2), but affect mostly its "intermediate" (see below) asymmetric conformations.

To understand better the association strength of different FGFR3 TM dimer conformations, rank them energetically, and estimate an energetic effect of the mutations, we performed free energy calculations for all the dimeric states in POPC bilayer using the umbrella sampling protocol (SI).[9] We also account separately for protein−protein, protein−membrane, and protein-water terms, which contribute to the total free energy of association (SI).[9] As seen in Figure 2, Arg or Glu substitutions almost do not change the dimerization free energy of the symmetric s1 model (−16 kcal mol^{-1}), where the both mutations are located on the dimer interface. At the same time, here we observe redistributions between the individual free energy terms. If in WT s1 dimer protein−membrane has strong unfavorable contribution into the total energy gain (Figure 2a), G380R mutation makes interactions with lipids favorable, while the energy gain for protein−protein term becomes positive (Figure 2c). In contrast, A391E decreases sufficiently the energy of protein−protein interactions and makes interactions with environment unfavorable (Figure 2e). For another symmetric conformation of the dimer (s2), where both mutated residues are exposed to lipids, the free energy gain is observed to be lower for mutant peptides as compared to the WT one. In the particular case of G380R, the free energy of s2 conformation is decreased by almost 6 kcal mol^{-1} as compared to WT due to more favorable dimer interactions with lipids (Figure 2c). As a result, the initial energy gap of about 8 kcal mol^{-1} between the conformations s1 and s2 (Figure 2b) becomes significantly smaller (~2 kcal mol^{-1}, Figure 2d). Similar to s1, A391E increases the efficiency of protein−protein interactions within s2 conformation (Figure 2e), but the total energetic effect in this case is less prominent and the energy gap between the two states remains significant (~4 kcal mol^{-1}, Figure 2f). Interestingly, we observe the effect of both mutations on the dimerization strength of the conformation s2, where the replaced residues are exposed to lipids and not

dx.doi.org/10.1021/ja4011942 | J. Am. Chem. Soc. 2013, 135, 8105−8108

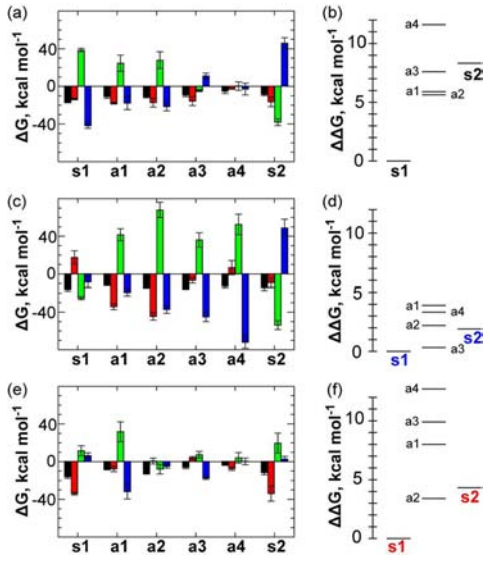

Figure 2. Association strength of various FGFR3 TM dimer conformations. (a,c,e) Dimerization free energies of different dimer models (black bars) and individual free energy contributions of protein−protein (red bars), protein−membrane (green bars), and protein−water (blue bars) interactions obtained for (a) WT, (c) G380R, and (e) A391E peptides. (b,d,f) Relative dimerization free energy diagrams depicting relative energy distances of different dimer conformations of (b) WT, (d) G380R, and (f) A391E peptides. In all cases, the free energy value obtained for the model s1 was taken as a reference point (equal to zero).

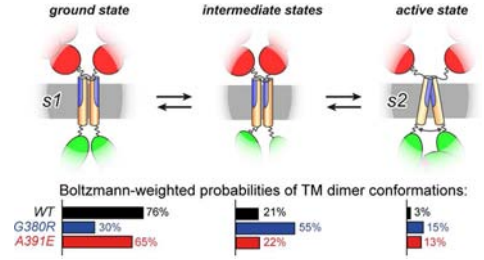

Figure 3. Role of TM mutations in activation of FGFR3. Putative "non-active" s1 conformation of the FGFR3 TM dimer has small helix−helix crossing angle, which promotes a symmetric configuration of the cytoplasmic domains (shown in green), thus resulting in autoinhibition of the receptor kinase activity.[11] FGFR activation requires antiparallel configuration of the kinase domains,[12] which can be easily achieved only when C-termini of the TM FGFR3 domains are spaced apart in a symmetric manner (similarly to EGFR kinase activation model).[13,14,15] The latter TM dimer configuration corresponds to its alternative symmetric s2 state. Asymmetric conformations of TM dimer can contribute to the transition between s1 and s2 TM dimeric states and supply an alternate activation of both kinase domains. G380R and A391E mutations in TM region of FGFR3 affect the transition pathway between s1 and s2 via repopulation of TM dimeric states that might contribute to activation efficiency of the receptor induced by either thermal "noise" (basal activity) or ligand binding. Extracellular, TM, and kinase domains of FGFR3 are shown with red circles, cylinders, and green ellipses, respectively. Blue and orange colors correspond to hydrophilic and hydrophobic regions of TM helices, respectively. The membrane is represented as gray hatching. Boltzmann-weighted probabilities of various TM dimeric states were estimated from the calculated association free energy values (Table S3).

involved in the helix−helix contacts. This view is consistent with previous modeling studies.[10]

Free energy estimation gives even more intriguing results, when it comes to different asymmetric states of the dimer in the membrane. For the WT dimer, most of such conformations (except a4, which has the smallest absolute dimerization free energy among the others and thus would occur with very low probability) have favorable protein−protein interactions (Figure 2a) and provide the free energy gain somewhat lower but close to that of s2, and thus, they are well separated energetically from the s1 (Figure 2b). From these data it is clearly seen that the free transition of the WT dimer from s1 to s2 conformation has low probability, and "intermediate" a1−a3 states are even more likely. Arg substitution decreases the dimerization free energy of all asymmetric conformations (Figure 2c). This corroborates strong structural effect of this mutation (see above). Interestingly, for all asymmetric conformations introduction of Arg makes dimer interaction with lipids unfavorable, while the opposite is true for protein−protein (a1, a2) or protein−water interactions (a3, a4) (Figure 2c). From the energy diagram it is clear that only a3 dimer has energy lower than s2. Taking into account the small energy gap between s1 and s2 conformations, we suppose that the spontaneous transition between these two states has higher probability than in the case of WT dimer, although "intermediate" asymmetric conformations are also very likely and might deplete the state s1 (Figure 3, see below). In contrast, A391E mutation increases the dimerization free energies for most of asymmetric conformations (except a2), mainly by making protein−protein interactions less favorable (Figure 2e). As a consequence, the population of s2 for Glu mutant should be much higher (Figure 3, see below) than in WT dimer due to two factors: smaller free energy of its own association and higher energies of alternative conformations (Figure 2f).

As follows from the results of the free energy calculations, s1 conformation of TM dimer of FGFR3 being the most favorable one (Figure 2b) very likely predominantly populates its putative nonactive ligand free state. In contrast, in such an unperturbed state of the receptor, dimer s2 is sparsely populated (Figure 2b). Indeed, for the modeled ensemble of FGFR3 TM dimer, the calculated Boltzmann-weighted probabilities of the first and the second symmetric conformations differ significantly: 76 and 3%, respectively (Figure 3, see SI for details). Thus, we reasonably suppose that s2 conformation of TM fragments corresponds to the active state of the dimeric receptor (Figure 3) and that only significant structural rearrangements of the extra-cellular domains taking place upon the ligand binding might facilitate transition from s1 to s2. Very recently, similar coupling of different symmetric TM dimer conformations to active and nonactive states of another receptor tyrosine kinase (epidermal growth factor receptor, EGFR) has been confirmed by application of combined experimental and MD simulations techniques.[14,15] According to our findings, we also claim that asymmetric dimer conformations (a1−a3) here might delegate their geometry for the intermediate receptor state(s), thus forming a hypothetical activation pathway.

Although we observe no effect of G380R mutation on the dimerization efficiency of the s1 conformation (assuming the systematic error of the approach, Table S3), this mutation significantly decreases the energy gap between s1 and s2 conformations (Figure 2d). Moreover, Arg substitution decreases dramatically the Boltzmann-weighted probability of the first symmetric conformation (predominant for WT) and increases the population of asymmetric dimer states (Figure 3). This observation can be interpreted as a structural rearrangement of G380R TM dimer as compared to WT that was previously

dx.doi.org/10.1021/ja4011942 | J. Am. Chem. Soc. 2013, 135, 8105−8108

suggested based on FRET experiment for both isolated FGFR3 TM dimer[6] and the full-length receptor.[16] Increasing of s2 population by 12% suggests higher probability of the "active" TM dimer as compared to WT that even without binding of the ligand might consequently promote amplification of the basal activity of the receptor (Figure 3). In addition, the global effect of G380R mutation on the membrane mode of TM dimer (e.g., partial emersion of the whole TM dimer toward the water−lipid interface) might also subsequently modulate function of the receptor associated with efficiency of ligand induced activation,[17] cross-phosphorylation, and down regulation. Particularly, slow down regulation is responsible for the signal prolongation of the mutant receptors, where the shifted membrane position of the TM helices might affect ubiquitination of FGFR3[18,19] However, the latter effects are associated with extra-membrane domains of the receptor, which are beyond the scope of the present study.

Similarly, the free energy of dimerization for A391E mutant TM peptides in predominant s1 conformation is the same as that for WTs, while the mutation increases significantly (by 3.2 kcal mol^{-1}, Table S3) the association strength in s2 state and reduces the gap between the both symmetric conformations (Figure 2f). To comment the deviation of the energetic effect of Glu substitution for the predominant s1 state from the experimental FRET data on TM fragments of FGFR3,[7] we should mention that the reported free energies are obtained exclusively for the particular dimer conformations, while the experimental data represent average properties of the conformational ensemble. In the latter case, we observe redistribution (Figure 3) between "ground" s1 (population is smaller by 9% then for WT) and "active" s2 states (population is higher by 10% then that for WT), which might be associated with higher basal activity of the mutant receptor.[5]

It is important to note that not only mutations can affect the energy distances between different FGFR3 TM dimer conformations. As we have shown previously, the dimerization strength can depend on the lipid environment.[9] For instance, in thinner and more flexible dimyristoylphospatidyl-choline membrane we observe smaller free energy gaps between s1 and s2 states of WT dimer as compared to the results in POPC bilayer (Figures 2a,b and S6).

In conclusion, in the present study we found a number of putative FGFR3 TM dimer conformations instead of just a single predominant structure usually available by NMR techniques. The predicted predominant state s1 of WT dimer agrees well with the experimental dimer structure obtained in parallel to our modeling (Figure S3), thus illustrating general validity of the computational approach. Why do RTKs TM domain dimers even need to adopt various conformations? Since the cell membrane is really heterogeneous in both composition and structural properties, a number of different conformations encoded in sequences of TM domains allow their better adaptation to the environment. Moreover, TM regions of RTKs transmit signals from the external receptor parts to cytoplasmic kinase domains that assumes conformational flexibility of TM dimers important for the receptor functioning. In the particular case of FGFR3, we proposed coupling of s1 and s2 symmetric conformations of TM dimer to the ground and active states of the receptor in the similar manner as it has been shown for EGFR.[14] Taking together the results obtained for two different members of RTK family, we reasonably assume that the conformational switch in the TM region can represent a general mechanism of activation of such receptors. The point mutations in FGR3 TM regions can induce conformational rearrangements of the dimer affecting its association strength in different states. Moreover, the free energy estimations suggest that the transition between "non-active" and "active" TM dimer conformations can proceed through different pathways for WT and mutant peptides, where particular intermediate conformations would be selected by the receptor according to its free energy landscape. We believe that the proposed mechanism of modulation of FGFR3 activity induced by TM mutations is also not unique and can be shared by other RTKs.

■ ASSOCIATED CONTENT

Supporting Information

Methods section and characterization data. This material is available free of charge via the Internet at http://pubs.acs.org.

■ AUTHOR INFORMATION

Corresponding Author

newant@gmail.com

Author Contributions

‖These authors contributed equally.

Notes

The authors declare no competing financial interest.

■ ACKNOWLEDGMENTS

Work was supported by the Ministry of Education and Science of the Russian Federation (MK-8439.2010.4; 07.514.11.4127; 14.514.11.4069), the Russian Foundation for Basic Research, and the RAS Programs "Basic fundamental research for nanotechnologies and nanomaterials" and "Molecular and Cellular Biology". Access to computational facilities of the Joint Supercomputer Center RAS (Moscow) and Moscow Institute of Physics and Technology is gratefully acknowledged.

■ REFERENCES

(1) Li, E.; Hristova, K. *Biochemistry* **2006**, *45*, 6241.
(2) Shiang, R.; Thompson, L. M.; Zhu, Y. Z.; Church, D. M.; Fielder, T. J.; Bocian, M.; Winokur, S. T.; Wasmuth, J. J. *Cell* **1994**, *78*, 335.
(3) Meyers, G. A.; Orlow, S. J.; Munro, I. R.; Przylepa, K. A.; Jabs, E. W. *Nat. Genet.* **1995**, *11*, 462.
(4) Webster, M. K.; Donoghue, D. J. *EMBO J.* **1996**, *15*, 520.
(5) Chen, F.; Degnin, C.; Laederich, M.; Horton, W. A.; Hristova, K. *Biochim. Biophys. Acta* **2011**, *1808*, 2045.
(6) You, M.; Li, E.; Hristova, K. *Biochemistry* **2006**, *45*, 5551.
(7) Li, E.; You, M.; Hristova, K. *J. Mol. Biol.* **2006**, *356*, 600.
(8) Han, X.; Mihailescu, M.; Hristova, K. *Biophys. J.* **2006**, *91*, 3736.
(9) Polyansky, A. A.; Volynsky, P. E.; Efremov, R. G. *J. Am. Chem. Soc.* **2012**, *134*, 14390.
(10) Zhang, J.; Lazaridis, T. *Biophys. J.* **2009**, *96*, 4418.
(11) Mohammadi, M.; Schlessinger, J.; Hubbard, S. R. *Cell* **1996**, *86*, 577.
(12) Bae, J. H.; Schlessinger, J. *Mol. Cells* **2010**, *29*, 443.
(13) Jura, N.; Endres, N. F.; Engel, K.; Deindl, S.; Das, R.; Lamers, M. H.; Wemmer, D. E.; Zhang, X.; Kuriyan, J. *Cell* **2009**, *137*, 1293.
(14) Endres, N. F.; Das, R.; Smith, A. W.; Arkhipov, A.; Kovacs, E.; Huang, Y.; Pelton, J. G.; Shan, Y.; Shaw, D. E.; Wemmer, D. E.; Groves, J. T.; Kuriyan, J. *Cell* **2013**, *152*, 543.
(15) Arkhipov, A.; Shan, Y.; Das, R.; Endres, N. F.; Eastwood, M. P.; Wemmer, D. E.; Kuriyan, J.; Shaw, D. E. *Cell* **2013**, *152*, 557.
(16) Placone, J.; Hristova, K. *PLoS One* **2012**, *7*, e46678.
(17) He, L.; Shobnam, N.; Wimley, W. C.; Hristova, K. *J. Biol. Chem.* **2011**, *286*, 13272.
(18) Monsonego-Ornan, E.; Adar, R.; Feferman, T.; Segev, O.; Yayon, A. *Mol. Cell. Biol.* **2000**, *20*, 516.
(19) Monsonego-Ornan, E.; Adar, R.; Rom, E.; Yayon, A. *FEBS Lett.* **2002**, *528*, 83.